

Frenetic steering in a nonequilibrium graph

Bram Lefebvre and Christian Maes

Instituut voor Theoretische Fysica, KU Leuven, Belgium*

Starting from a randomly-oriented complete graph, an algorithm constructs equally-sized basins of attraction for a selection of vertices representing patterns. For a given driving amplitude, a random walker preferentially follows the orientation, while the nondissipative activity is considered variable. A learning algorithm updates the time-symmetric factor in the transition rates, in order that the walker will quickly reach a pattern and remain there for a sufficiently long time, whenever starting from a vertex in its basin of attraction. No use is made of a potential or cost function where patterns would correspond to local minima, but the nonequilibrium features of the walk are essential for frenetic steering.

I. INTRODUCTION

Biological functioning is closely dependent on nonequilibrium conditions. More specifically, for what is probably the most complicated system on Earth, it is rather easy to verify that the human brain acts far from equilibrium. The evidence covers various levels of description, starting at the smallest scales of individual neurons and their nonequilibrium dynamics [1]. On the other end, using whole-brain imaging, large-scale nonequilibrium dynamics can be detected as well [2]. That should not be surprising, as the nonequilibrium dynamics of biological systems are required to avoid maximum entropy states, i.e., postponing thermal death by constant energy consumption and heat dissipation, [3].

In fact, the brain is one of the most demanding open systems in the body: fast synaptic signaling of neurons is metabolically expensive, e.g. from the transport of electric charges through pumps, [4, 5]. Even though the human brain constitutes only 2% of the body weight, the energy-consuming processes that ensure proper brain function account for approximately 25% of total body glucose-utilization, taking 20% of the body's oxygen supply at rest [6, 7].

* christian.maes@kuleuven.be

Also directly by inspecting time-series of the brain and neuronal activity, the breaking of time-reversal symmetry has been established. In [2, 8] (using a similar method to [9]), it was found that brain activity time series recorded during the conscious state significantly differ from the inverted version of the same data; that was not the case for unconscious states. It supports the idea that when the brain dynamics is chemically or physically farther from equilibrium, the recorded time series signals are irreversible. A lower level of consciousness appears to bring it closer to equilibrium and the signal also becomes more time-symmetric. In particular, the electrocorticography signals from non-human primates under different levels of consciousness show that temporal irreversibility of neural dynamics relates to different states of consciousness, [10].

Indeed, if the physical or cognitive tasks become more demanding, the brain produces more entropy. Yet, interestingly, the metabolic rate is only increased by about (not more than) 10% when the brain is stimulated, as has been demonstrated by imaging experiments [11]. As proposed by Raichle and Mintun in [12], the latter result suggests that the intrinsic activity of the brain, which counts as the baseline neural activity, can be as significant as, if not more than, acquiring new information and responding to changing contingencies. Following that line of thinking, in what follows we fix the metabolic rate at a high level, i.e., the irreversible work done by the chemical fuel to transport activity between two “close” regions is considered given. Yet, the process of storing and memorizing patterns will involve frenetic (i.e., nondissipative and time-symmetric) components while taking place against that background of constant driving.

In nonequilibrium models, adding a potential to guide the system towards stored patterns does not work as used in traditional setups of neural networks and machine learning. In other words, when time-reversibility is absent in the open system stationary dynamics, we should not expect a thermodynamic free energy landscape, cost, or loss function to guide the variational relaxation to a nearby pattern. Even the traditional methods of irreversible thermodynamics, where fluxes are linear functions of driving forces, would not do as they typically do not take into account fluctuations and nonlinearities arising from digital processing. However, the positive news is that for nonequilibrium processes, even in the Markov approximation, time-symmetric kinetic parameters start to matter greatly; see e.g. [13–15]. In fact, population selection, kinetic proofreading, error-correcting, and

pattern recognition are different melodies on the same theme. They all occur in biological systems and under nonequilibrium driving, e.g. in the form of ATP hydrolysis, they make use of time-symmetric kinetics to obtain the required goal. Those kinetic parameters are invisible in the stationary (equilibrium) population statistics for detailed balance dynamics but they can make all the difference out of equilibrium.

In the present paper, we take seriously the nonequilibrium condition of neuronal networks but we do not try to model neurons and their connections directly. Rather, we take a coarse-grained view and think of vertices in a complete graph as possibly different locations of activity. We will have a random walker hopping to neighboring vertices to represent the transport of that activity, e.g. realized by neuronal firing and charge transport. Its arrival at a pattern vertex is meant to correspond to the cognitive activity of recovery. Quite naturally, in our setup as in real brains, no direct image of a pattern is simply copied on a neuronal configuration.

Far from providing a neurophysiological scheme, the goal of the paper is to create a novel context of ideas for pattern storage and recovery in bioactive systems. There are two learning steps. First, the brain creates basins of attraction for the various patterns, and second, it learns to connect the locations in each basin with a pattern.

The next section specifies the problem to be solved, which is basically about classifying states and finding the representative pattern in each class without gradient dynamics. The first learning step, about generating basins of attraction, is explained in Section III. Section IV gives the method of frenetic steering. The performance of the algorithm is discussed in Section V. An Appendix presents some simple examples and gives more details about the algorithm. The complete code can be found in [16].

II. SETTING THE PROBLEM

We make the problem specific by choosing the complete graph with N vertices. That is a simplification for exploring the ideas and at the same time, a complete graph is the most symmetric point of departure. We randomly orient every edge $\{x, y\}$ by assigning, independently, variables $\sigma(x, y) = -\sigma(y, x) \in \{-1, +1\}$ to its two orientations $(x, y) : x \rightarrow y$ and $(y, x) : y \rightarrow x$. When $\sigma(x, y) = +1$, we say that the orientation $x \rightarrow y$ is preferred. In

that way, we may visualize the preferred direction by arrows assigned to every edge of the complete graph, making it into a tournament.

At the same time, we put $s(x, y) = \varepsilon \sigma(x, y)$, $s(y, x) = -s(x, y)$ with $\varepsilon > 0$ giving the magnitude of a nonequilibrium driving. Those choices remain unaltered during all of the constructions and learning. In addition, we attach an unoriented weight $a(x, y) = a(y, x) > 0$ to each edge, which, in contrast, will be altered during learning. They realize synaptic strengths on a coarse-grained level.

Next, we define a random walker X_t on the graph. It is interpreted as transmitter of firing activity. The walker has transition rates $k(x, y) > 0$ to hop over the edge $x \rightarrow y$ with

$$\sqrt{k(x, y)k(y, x)} = a(x, y), \quad \log \frac{k(x, y)}{k(y, x)} = s(x, y) \quad (1)$$

The weights $\{a(x, y)\}$ are the time-symmetric activity parameters of the random walker. They are variable and will be updated to steer the random walker.

The goal for the walker is to reach a pattern, interpreted as a condition of cognitive recall. More precisely, we randomly select $k > 1$ patterns, i.e. k different vertices $\{x_1, x_2, \dots, x_k\}$ on the graph, which serve as targets for this random walker. The problem is to train the walker by adapting its time-symmetric activity parameters so that the following holds:

- Randomly draw a vertex u and start the random walker from $X_0 = u$. We want that there is a pattern x_i so that with high probability $X_T = x_i$ at time T and that the residence time-interval $I = [t_i, t_f] \ni T$ for which $X_t = x_i, \forall t \in I$, has a duration $|t_f - t_i| \geq \tau$ at least τ . We then say that u is in the basin of attraction B_i of pattern x_i .
- We want that for each pattern $x_i, i = 1, \dots, k$, the number of vertices $|B_i|$ in its basin scales like N/k .

Moreover, altering the time-symmetric activity parameters $\{a(x, y)\}$ will be done iteratively, via supervised learning, whereby the initial value is taken uniform: $a(x, y) = a, \forall x, y$ for some $a > 0$.

The first problem is to divide the network into different regions (“colors”) belonging to one particular pattern. Depending on the random orientations, the network stores the patterns in different basins. In that first learning step, we run an algorithm, again containing some random decisions, for the successful decomposition of the graph into basins of attraction B_i ,

given any selection of patterns and for “any” (random) realization of the orientation of the complete graph. We start with that in the next section.

The second (supervised) learning step towards recovery (in Section IV) wants to achieve that starting the random walker from a vertex in B_i , it arrives ‘fast enough’ (after at most a time T) in x_i and stays there for a good while (at least a time τ). One should imagine here that when the walker arrives at the pattern, it “lights up” announcing the “color” of the vertex in which the walker started. In that interpretation, upon stimulating a region of the network (start of the random walk), after a short time, we find out to what pattern it belongs.

The algorithms are implemented in python [17], where the library numpy [18] was used for general calculations and the library matplotlib [19] enabled to investigate the performance of the algorithms. The source code of the implementations of the algorithms can be found at [16].

In Section V we run the algorithms and check their performance, also as a function of N, k and (what will be called) the training set size. Finally, in the conclusion Section VI, we give an outlook including more interpretation.

III. DISENTANGLING THE BASINS OF ATTRACTION

The goal of the disentangling algorithm is to decompose the randomly-oriented complete graph into basins of attraction. We keep in mind Fig. 1 as the ideal scenario, where each pattern is the hub and attractor of loops and oriented trees, selected from the randomly oriented complete graph. For the next step of teaching the random walker, it enables to start from there by setting $a(x, y) = 0$ for certain edges $\{x, y\}$. In other words, we can view the disentangling algorithm as making decisions about which arcs of the digraph (of positively oriented edges) to keep and which to remove. Note that our disentangling is not merely a clustering or coloring of the graph as we wish to have each cluster associated with a unique pattern toward which all edges are oriented. In other words, the leading idea of disentangling is to provide fast lanes to each pattern,

Having the random orientations in the complete graph, we keep the preferred directions. What we obtain is a tournament, i.e., an oriented complete graph. It is of course a directed graph (digraph). We denote a tournament by \mathcal{T} , the vertices by $V(\mathcal{T}) = V$, and the set of

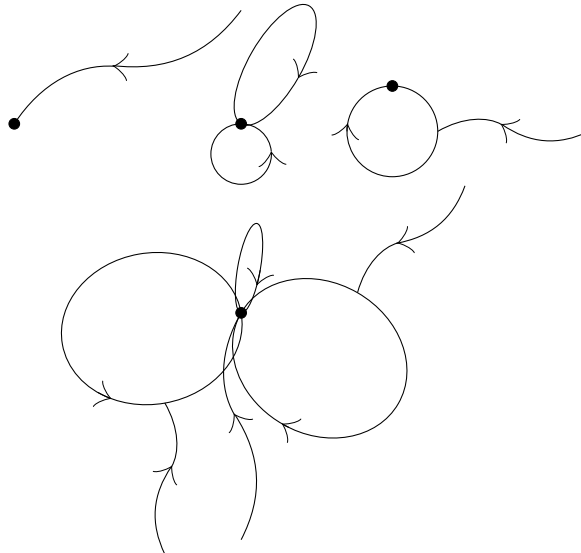


FIG. 1. The desired disentangling where each pattern (here, $k = 4$) has become the center and attractor of oriented loops and hairs.

arcs (edges in the preferred direction) by $A(\mathcal{T}) = A$.

In each step of the disentangling algorithm, we will have a tournament but with a variable number of vertices. Before that, however, let us repeat some elementary notions; we refer to [20, 21] for standard results in graph theory.

A *path on a digraph* is a sequence of distinct vertices so that for every two subsequent vertices y_i and y_{i+1} , $(y_i, y_{i+1}) \in A$. For a cycle on a digraph the first and the last vertices in the sequence must be the same: a *cycle* (on a digraph) of length ℓ is a sequence of vertices $y_i \in V$, $0 \leq i \leq \ell$, which are all distinct except for the end and start, and for every two subsequent vertices y_i and y_{i+1} , $(y_i, y_{i+1}) \in A$.

A digraph is called strongly connected or strong if for every pair of vertices $x, y \in V$, there exists both a path from x to y and a path from y to x . Whether a subtournament is strong will be checked at each step of the algorithm. A strong tournament must contain a cycle including all vertices of the tournament (called, a Hamilton cycle). If such a Hamilton cycle exists, then the tournament is strong. So we check if the subtournament is a strong tournament by searching a Hamilton cycle and that we do with an implementation of Manoussakis' algorithm. In Appendix A 1 we mention the most important ideas used in Manoussakis' algorithm. The full algorithm can be found in [22].

For a strong tournament \mathcal{T} , Moon's theorem applies: for every vertex $x \in V(\mathcal{T})$ and every

integer ℓ for which $3 \leq \ell \leq |V(\mathcal{T})|$ there exists a cycle of length ℓ in \mathcal{T} . The proof of Moon's theorem points towards an algorithm to find these cycles. In Appendix A 2 we mention the most important ideas. The full proof of the theorem can be found in [20] p. 16.

We next explain the algorithm and start with the very first step. We have our original oriented complete graph and of the N vertices we have selected k pattern vertices. The latter are numbered, and we start from pattern vertex x_1 . We consider the new tournament obtained from removing all vertices x_2, \dots, x_k and all their in- and outgoing edges from the original complete graph. We check whether that new tournament is strong using Manoussakis' algorithm mentioned above. For the moment we assume it is. Then, we find a cycle of length three containing x_1 and add the 2 new vertices and the arcs of the cycle to the basin B_1 .

Next is pattern vertex x_2 and we remove all vertices so far labeled to be in a different basin. In that step, it means to remove x_1 and its two added vertices and also x_3, x_4, \dots, x_k are removed with again all their in- and outgoing edges. We again remain with a tournament, and we check whether it is strong. If yes, which we suppose for now, we find a cycle of length 3 with two additional vertices and corresponding arcs that we label to be added to the basin B_2 of the second pattern. We continue like that and when we have finished with pattern vertex x_n , we return to pattern vertex x_1 . We delete of course every vertex and its edges destined for a particular basin B_i , $i = 2, \dots, k$, and we get a tournament for which we check whether it is strong (which we continue to suppose). Then, we find a cycle of length 4, and add its vertices (some of which could already have been labeled this way) and arcs to belong to basin B_1 .

More generally, at each step, we take a subtournament of the oriented complete graph by removing all vertices that are elements of the other basins from the complete tournament. First, we check if this subtournament is a strong tournament. If it is a strong tournament we look for a cycle and add its vertices and arcs to the basin. If it is not a strong tournament we skip this basin and just go to the next basin. Note that of course when it is not a strong subtournament our desire for the basins to be of similar size can become compromised. The length of the cycle we look for is one more than the length of the cycle we added last to the basin and the length of the first cycle we look for is 3, which is of course the shortest possible cycle. With Moon's theorem, we are always certain that there exists such a cycle.

With this algorithm, while we are looking for a cycle, we are not concerned whether the vertices of the cycle are already contained within the basin or not, which also helps to keep the algorithm simple. The minimal size of the basin is the length of the cycle that was added last, and that increases as the algorithm keeps running. At the end of the algorithm, we remove all arcs that were not part of a cycle that was found.

It is possible that at the very beginning, no subtournament is strong, i.e., that all subtournaments obtained by removing all pattern vertices except for one, are not strong. In that case, all the basins contain only their pattern vertices. Yet, from the moment one of these subtournaments is strong all vertices will eventually be part of some basin because in that case there is always a strong subtournament, namely the one for which the last found cycle was found, and the length of the cycle we look for a certain basin increases every time we find a new cycle so that it is inevitable that every vertex is at some point part of a basin.

After the above steps in the algorithm have finished we eliminate all cycles that do not contain a pattern. We explain this in Appendix B. At the end, we set $a(x, y) = a(y, x) = 0$ for every arc (x, y) that was removed.

In Appendix D 1 we give an example of the steps made by the disentanglement algorithm executed on the tournament in Fig. 5. The performance of the algorithm is discussed in Section V A.

To have a good idea of what the disentangling is about, we refer to Fig. 1. We have added hairs (which we ignore in the text) to show better the idea: each pattern is supposed to be a hub where loops get together, each possibly having trees connected to them. The (positive) orientation is toward the pattern or toward a loop. All other arcs are removed. In that way, the graph is prepared for the next step.

IV. FRENETIC STEERING

We come to the second learning step, starting after the disentangling. Indeed, after the disentanglement we have divided the graph into “rooms with a different color”, each belonging to a unique pattern; see Fig. 1. When starting anywhere in one of those rooms,

we want to recall the corresponding pattern. In order to achieve that, we alter the activity parameters during a learning process; they will no longer be uniform. Note that we do not want to inspect the basin of attraction globally and decide on a specific choice of time-symmetric activities in each case. Rather, we wish to teach a random walker locally how to explore the basin to reach the pattern at the right time and for the right amount of time.

The general philosophy is obviously that the transition rates leaving a pattern should be small and that for each state in a basin there should be (a) fast path(s) ‘toward’ the corresponding pattern. Supervised learning is to generate paths of the random walk and, if a path is not desirable, to change the activity parameters in a strategic way. That is what we call frenetic steering, and we refer to Appendix C for some more background.

We choose to generate paths by randomly picking an initial state and letting the system evolve until it leaves the state it was in at time T . The number of times we do this we call the training set size n .

We know that a successful path must at time T be in the pattern and stay long enough there. For the training we want the system to arrive in the pattern in a time less than or equal to T and once it has arrived in the pattern to not leave before the time T and to stay longer than the minimal residence time τ .

What is left to decide is the value with which we want to increase or decrease the activity parameters. We choose that value to be proportional to the current value. Introducing a learning rate R , where $0 \leq R \leq 1$, we define the adjustment to the symmetric part as follows:

$$\Delta a(x, y) = \begin{cases} (1/R - 1)a(x, y) & \text{when increasing} \\ (R - 1)a(x, y) & \text{when decreasing} \end{cases} \quad (2)$$

We distinguish three ways in which a path can be unsuccessful.

(1) the walker has at a time smaller than or equal to T left the pattern:

We decrease the activity parameters for all the transitions in the path leaving the pattern which are in the direction of the driving.

(2) the walker never visited the pattern before or at time T :

For every state in the path, we look at the next state in the path. If this next state in the

path is in the direction of the driving, we increase the activity parameters for the transition from the original state to this next state. If the next state in the path is against the direction of the driving, then we increase the activity parameters for all the transitions leaving the original state which are in the direction of the driving. There is a special case for the last state in the path, which does not have a next state of course. For the last state of the path we also increase the activity parameters for all the transitions leaving this state which are in the direction of the driving. We take care to not increase the same activity parameters multiple times during the handling of this case.

(3) the walker has never left the pattern before time T and was present in the pattern at time T but the actual residence time was smaller than the minimal residence time τ : We decrease the activity parameters for all transitions in the direction of the driving from the last state the system is in to a state outside the pattern.

In Appendix D2 we give examples of generated paths and describe the actions that are taken by the frenetic steering algorithm when it generates them. The performance of the algorithm is discussed in Section VB.

To summarize, the input parameters for the entire algorithm are

- the travel time T and residence time τ ,
- driving value ε and initial value for the time-symmetric activity parameters a ,
- learning rate R , and
- training set size n , complete graph size N and pattern number k .

In what follows we take the values $T = 1$, $\varepsilon = 5$, $R = 0.5$, $\tau = 0.2$, $b = 5$, and n will be a fraction or proportional to N . We investigate the performance as a function of N, k, n , while sometimes fixing k/N .

V. PERFORMANCE

A. Performance of disentangling

For reasons of symmetry, we like the basins to be of similar size. To check, we generate 10 strong tournaments (orientations of the complete graph) and for each of these tournaments, we do the disentanglement 10 times. We thus obtain 100 disentangled systems. The size of a basin $|B|$ is the number of its vertices, not including the pattern vertex, and with the applied algorithm we reach an average size equal to $N/k - 1$.

As a first example we take $N = 50, k = 5$. The average size of a basin is 9 in this case. For the 100 disentangled systems, the distribution of the size of the smallest basin is given in the table below:

size smallest basin	5	6	7	8	9
frequency	2	23	43	31	1

As a measure of performance, we consider the average difference in the sizes of the basins

$$\frac{1}{k(k-1)/2} \sum_{i=1}^k \sum_{j=i+1}^k ||B_i| - |B_j|| \quad (3)$$

Fig. 2 shows the average of the average difference in the sizes of the basins for the 100 disentangled systems mentioned above for systems with 1000 states as a function of the number of patterns. We see that it quickly decreases with an increasing number of patterns and then oscillates. An explanation for this is given in Appendix E. We see that the average difference is typically low. The average difference in the sizes of the basins stays more or less the same at a value of a bit less than 2 for $N = 10 - 100$ where $N/k = 10$. The average size of a basin is 9 in this case.

We also consider the relative average difference in the sizes of the basins, meaning to multiply 3 by $k/(N - k)$. In Fig. 3 we show this relative average difference in the sizes of the basins for systems with 5 patterns as a function of the number of states. Again, what we show in the plots is the average of this average for the 100 disentangled systems mentioned

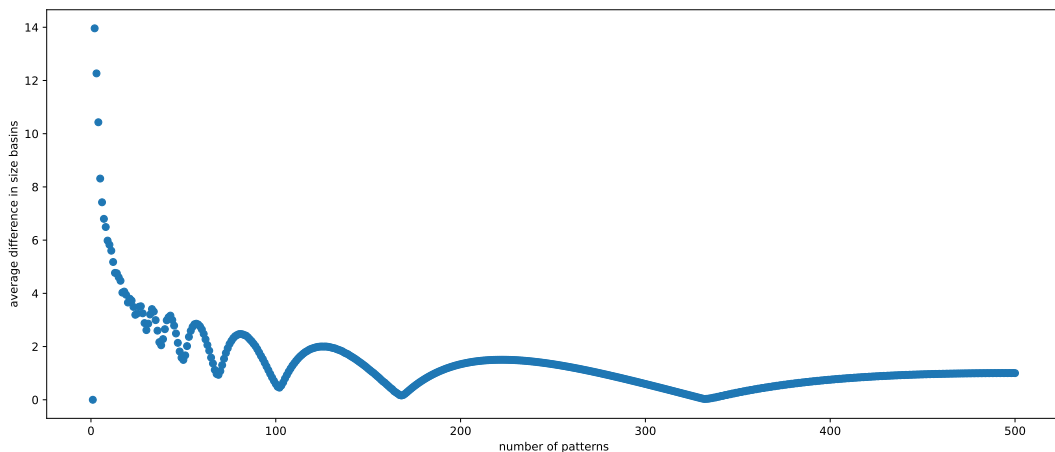


FIG. 2. Average difference in the sizes of the basins for the disentanglement step for systems with 1000 states as a function of the number of patterns.

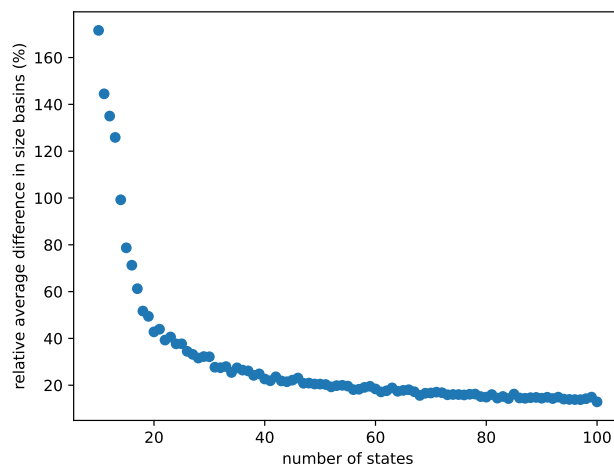


FIG. 3. A relative average difference in the sizes of the basins, i.e., 3 divided by $N/k - 1$, for systems with 5 patterns as a function of the number of states.

above. In general, the disentangling gets worse when k/N gets larger.

The time it takes for the disentanglement algorithm to finish on a modern personal computer is around 40 ms for a strong tournament with $N = 100, k = 5$. We found that the algorithm spends most of its time eliminating the cycles that do not contain a pattern and checking whether a tournament is strong. For the parameter configurations we have

investigated, the algorithm spends less than 20% of its time on the rest. The algorithm would run faster if we would abandon the condition that the subtournament must be strong. That check is not essential: we can still try to find a cycle even though we have no guarantee that there is one for every specific length.

B. Performance of frenetic steering

To measure the performance of the random walk obtained after training, we start with each state of the system and we look if the system is in the pattern at time T and stays long enough in the pattern. If that is the case a success is recorded, otherwise a failure. We generate 10 strong tournaments and for each of those, we do the disentanglement. We thus obtain 10 disentangled systems. On each of those 10 disentangled systems, the frenetic steering is executed and we examine the average performance of these 10 random walks. The results do not depend on the travel time, because the time scaling can be set by choosing an appropriate value a for the initial value of the time-symmetric activity parameters. Choosing

$$a = \frac{20}{T} \exp\left(\frac{-\varepsilon}{2}\right) \quad (4)$$

gives a decent performance. Increasing the driving value ε leads to better results. In what follows we work with the values: $T = 1$, $\varepsilon = 5$ so that $a \simeq 1.64$. We also take $R = 0.5$ in (2) and duration $\tau = 0.2$.

In Fig. 4 we plot the performance for systems with 1000 states as a function of the number of patterns for different values of the training set size n . For every value of n the performance increases with an increasing number of patterns. The main reason is that the basins become smaller when the number of patterns increases. Then indeed, there are fewer cycles for each basin which means there are fewer arcs that have the pattern as start or end vertex. That makes the rate to leave a pattern smaller.

Naturally, the performance is higher for higher values of n ; see Fig. 4. Going to large training set size, the performance gets close to perfect. For systems with a number of states ranging from 10 to 100 where $N/k = 10$, performance is between 95% and 96% when the training size reaches $n = 4N$. For the same range in the number of states but with $N/k = 5$, the performance lies in a very close range just above 97%. For these estimates of the average

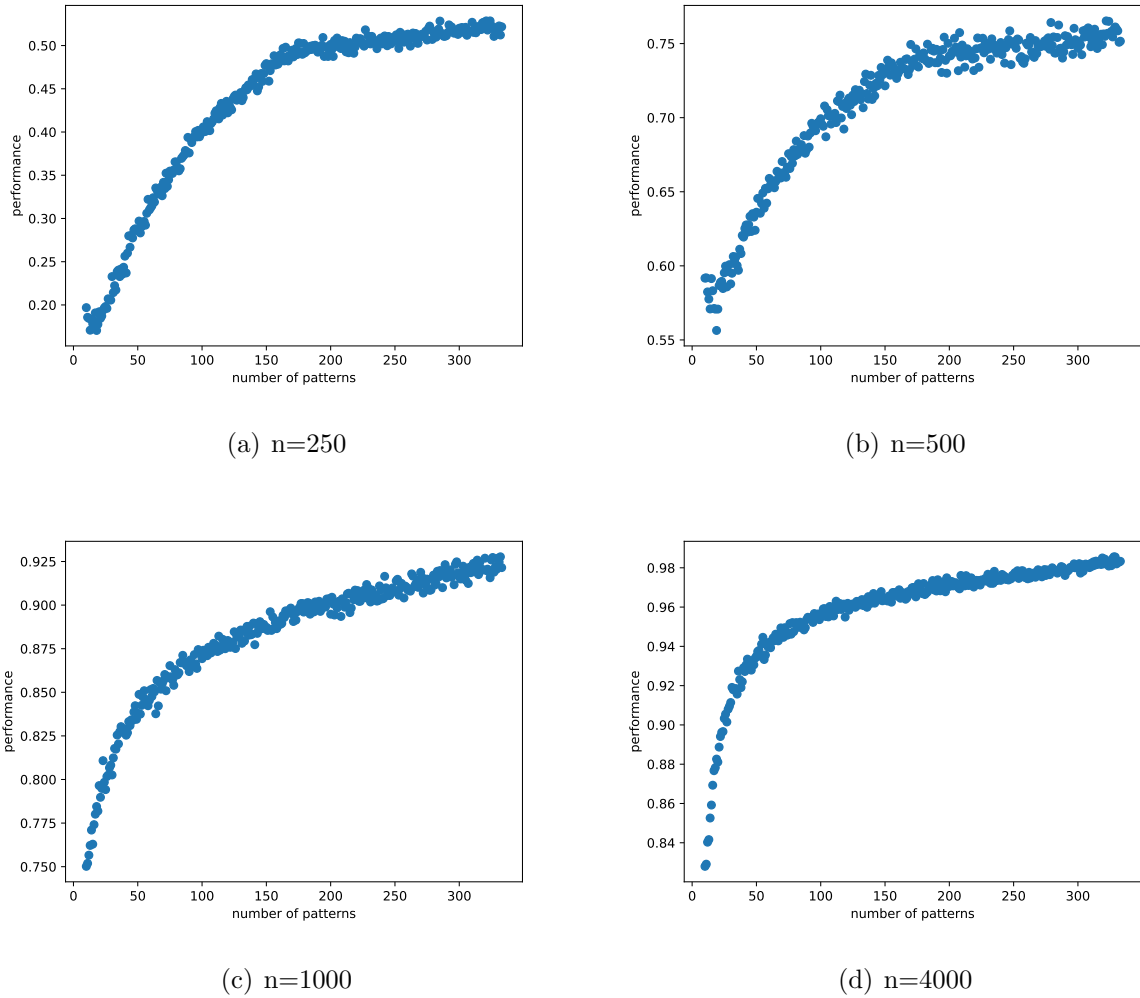


FIG. 4. Performance of the frenetic steering algorithm for systems with $N = 1000$ states as a function of the number of patterns for different values for the training set size n .

performance, we generated 10 strong tournaments and for each we did the disentanglement 10 times, so we got 100 disentangled systems. On each of those 100 disentangled systems, we started with each state of the system 100 times and checked whether the walker is in the pattern at time T and stays there long enough (for a time τ).

As a final remark, the time it takes for the algorithm to finish on a modern personal computer is around 200 ms for a disentangled system obtained from a strong tournament with 100 states and 1 pattern. The algorithm spends most of its time generating a path. For the parameter configurations, we have investigated this was more than 80% of the total

time.

VI. CONCLUSION

The morphology or physical chemistry of the brain is not leading to anything intelligent when passive. Instead, in biological information–processing, we are dealing with nonequilibrium systems, well-outside the perturbative regime of close-to-equilibrium considerations.

In the present paper, we give up the idea that patterns are stored “energetically,” as parameters in the interaction potential between neurons. We have introduced the concept of frenetic steering for the recall of a pattern. In the first learning step, the disentangling models the nonlocal division of brain regions, where each component connects various neuronal conditions. They are obtained starting from random but active wiring of the brain. Once the regions get formed, the frenetic steering organizes the recall in each region, in the spirit of the Hebb rule where the synaptic strength between neighboring vertices or cells that are part of a signaling pathway are increased. Indeed, the frenetic steering is making changes to the time-symmetric activity parameters in the transition rates. The time-symmetric parameters give weights to connectivities and they are able to modify the occupation statistics exactly because of the (random) background driving, [13, 15].

Giving an alternative to (stochastic) gradient evolutions along free energy landscapes, where patterns are local minima, is a difficult challenge. The present paper worked out a conceptual scheme and proof of principle for an alternative where we take advantage of the nonequilibrium condition to steer the firing paths by adapting time-symmetric reactivities. For further improvements and extensions, we have to look mostly at the disentanglement algorithm. The assumptions about the oriented complete graph are not essential but have made the algorithm easier to implement. For example, we can work with patterns containing multiple vertices, or we can add multiple hairs to the cycles, obtaining a decomposition as in Fig. 1. In general, for the frenetic steering, recall is successful when the training set size or/and the number of patterns is high enough.

Acknowledgment: Part of this work was started by Victor Kermans, [23], during his

Master thesis with CM.

- [1] D.A.R. Sakthivadivel. Characterizing the non-equilibrium dynamics of a neural cell. arXiv:2102.09146v1 [q-bio.NC].
- [2] C. W. Lynn, E. J. Cornblath, L. Papadopoulos, M. A. Bertolero, and D. S. Bassett, Broken detailed balance and entropy production in the human brain. *PNAS* **118** (47) e2109889118, (2021).
- [3] E. Schrödinger, *What is Life?* Cambridge University Press, 20th printing 2017 edition, 1967.
- [4] J. Karbowski, Metabolic constraints on synaptic learning and memory. *Journal of Neurophysiology*, 122(4):1473-1490, 2019.
- [5] J. Karbowski, Energetics of stochastic bcm type synaptic plasticity and storing of accurate information. *Journal of computational neuroscience*, 2021.
- [6] I. Allaman and P. J. Magistretti. Chapter 12 - brain energy metabolism. In L. R. Squire, D. Berg, F. E. Bloom, S. du Lac, A. Ghosh, and N. C. Spitzer, editors, *Fundamental Neuroscience (Fourth Edition)*, pages 261-284. Academic Press, San Diego, fourth edition edition, 2013.
- [7] L. W. Swanson. Chapter 2 - basic plan of the nervous system. In L. R. Squire, D. Berg, F. E. Bloom, S. du Lac, A. Ghosh, and N. C. Spitzer, editors, *Fundamental Neuroscience (Fourth Edition)*, page 36. Academic Press, San Diego, fourth edition edition, 2013.
- [8] G. Deco, Y. Sanz Perl, J. D. Sitt, E. Tagliazucchi, M. L. Kringelbach, Deep learning the arrow of time in brain activity: characterising brain-environment behavioural interactions in health and disease. bioRxiv 2021.07.02.450899.
- [9] A. Seif, M. Hafezi, and C. Jarzynski, Machine learning the thermodynamic arrow of time. *Nature Physics* 17, 105–113 (2021).
- [10] L. de la Fuente, F. Zamberlan, H. Bocaccio, M. Kringelbach, G. Deco, Y. Sanz Perl, and E. Tagliazucchi, Temporal irreversibility of neural dynamics as a signature of consciousness. *Cerebral Cortex*.
- [11] R. G. Shulman and D. L. Rothman. Interpreting functional imaging studies in terms of neurotransmitter cycling. *Proceedings of the National Academy of Sciences*, 95(20): 11993-11998, 1998.

- [12] M. E. Raichle and M. A. Mintun. Brain work and brain imaging. *Annual Review of Neuroscience*, 29(1):449-476, 2006.
- [13] C. Maes, Frenesy: Time-symmetric dynamical activity in nonequilibria. *Physics Reports* 850, 1-33 (2020).
- [14] M. Baiesi and C. Maes, Life efficiency does not always increase with the dissipation rate. *Journal of Physics Communications* 2, 045017 (2018).
- [15] C. Maes, Non-Dissipative Effects in Nonequilibrium Systems. *SpringerBriefs in Complexity*, 2018.
- [16] https://github.com/bramlefebvre/frenetic_steering
- [17] G. Van Rossum, G. and F.L. Drake, Python 3 Reference Manual, Scotts Valley, CA: CreateSpace, 2009.
- [18] C.R. Harris, K.J. Millman, S.J. van der Walt, *et al.* Array programming with NumPy. *Nature* 585, 357–362 (2020).
- [19] J.D. Hunter, Matplotlib: A 2D Graphics Environment, *Computing in Science & Engineering*, vol. 9, no. 3, pp. 90-95, 2007
- [20] J. Bang-Jensen and G.Z. Gutin, Digraphs: Theory, Algorithms and Applications. *Springer Monographs in Mathematics*. Springer London : Imprint: Springer, London, 2nd ed. 2009. edition, 2009.
- [21] D. B. West, Introduction to graph theory. Pearson Education, Inc., First Indian reprint, 2002.
- [22] Y. Manoussakis, A linear time algorithm for finding hamiltonian cycles in tournaments. *Discrete Applied Mathematics*, 36(2):199-201, 1992.
- [23] V. Kermans and C. Maes, Towards nonequilibrium aspects for neural networks. KU Leuven. Faculteit Wetenschappen. 2021. url
- [24] P. Hell and M. Rosenfeld, The complexity of finding generalized paths in tournaments, *J. Algorithms* 4 (1982) 303-309.
- [25] C. Maes and K. Netočný, *Heat bounds and the blowtorch theorem*. *Annales Henri Poincaré* 14(5), 1193–1202 (2013).
- [26] C. Maes, K. Netočný and W. O’Kelly de Galway, *Low temperature behavior of nonequilibrium multilevel systems*. *Journal of Physics A: Math. Theor.* 47, 035002 (2014).
- [27] R. Landauer, *Inadequacy of entropy and entropy derivatives in characterizing the steady state*. *Physical review A, Atomic, molecular and optical physics*, 12(2), 636–638, (1975).

- [28] F. Khodabandehlou, C. Maes, K. Netočný, Trees and forests for nonequilibrium purposes: an introduction to graphical representations. *J. Stat. Phys.* **189** (3), (2022).

Appendix A: Manoussakis' algorithm and Moon's theorem

We mention the most important ideas used in the proof of Moon's theorem and Manoussakis' algorithm. We use the expression that a vertex x dominates a vertex y when $(x, y) \in A$.

1. Manoussakis' algorithm

Manoussakis' algorithm wants to construct a Hamilton cycle. It starts by using an algorithm to find a Hamilton path [24]. The main idea there is that binary sorting does not (need to) use the transitivity property of a totally ordered set. We can use binary sorting for the order relation associated with a tournament to find a Hamilton path. Using this Hamilton path $y_1 \dots y_m$, Manoussakis' algorithm first finds the largest index i for which $y_1 \dots y_i y_1$ is a cycle. The algorithm then continues by induction by looking at the first vertex of the Hamilton path that is not part of the cycle. It is possible that this vertex dominates a vertex of the cycle. In that case, this vertex can be fitted within the existing cycle, so that we get a cycle of length one more than the existing cycle. If the first vertex of the Hamilton path that is not part of the cycle does not dominate a vertex of the cycle, then we look for the first one that does, call it y_k , and then we can fit the vertices of the Hamilton path that are not part of the cycle with index up to and including k together in that order in the existing cycle. This continues until a Hamilton cycle is obtained. If at some point the algorithm cannot continue, there is no Hamilton cycle. The full algorithm can be found in [22].

2. Moon's theorem

A tournament is reducible if its vertices can be separated into two non-empty subsets, A and B , such that every edge that joins a vertex in A to one in B is an arc towards the vertex in B . The basis for the arguments used in Moon's theorem is the fact that a strong tournament is equivalent to an irreducible tournament. The theorem is proven by induction. First, it is shown that for every vertex a 3-cycle exists containing this vertex. Then, given a cycle, it is possible that there are vertices outside the cycle that dominate some vertices in the cycle and are dominated by the other vertices in the cycle. Any of these vertices can be fitted within the existing cycle so that we get a cycle of length one more than the existing cycle. Otherwise, some vertices outside the cycle dominate every vertex in the cycle and the

other vertices outside the cycle are dominated by every vertex of the cycle. In that case, we can pick 2 vertices outside the cycle to replace one vertex in the cycle, so that again we get a cycle of length one more than the existing cycle. The full proof can be found in [20], p. 16.

Appendix B: Eliminating cycles

In the algorithm for disentangling the complete graph, we eliminate redundant cycles that do not contain the patterns.

We order the vertices that are not patterns, and we denote them by $y_{1,i}$ with $i = 1, \dots, N - k$. We start with a path that has length 1, which is a vertex: call it $y_{1,1}$. Next, we look at the vertices $z \in V$ that are not patterns, for which $(y_{1,1}, z) \in A$ (from here on, we call them forward vertices) and we order them and name them $y_{2,i}$ with i an integer starting from 1 and ending at the number of vertices z for which the above holds. For each of them, we create a new path that now looks like $(y_{1,1}, y_{2,i})$. The first index of these symbols is clear; it is the index in the path of the associated vertex. Now we first continue with the path $(y_{1,1}, y_{2,1})$ and again look for forward vertices: vertices $z \in V$ that are not a pattern vertex for which $(y_{2,1}, z) \in A$ and so on in the same way as above. In the beginning, we always continue with the path which has, as the last vertex, the first vertex in the newly found forward vertices. At some point, one of two things happens. It may be that we encounter a forward vertex that is already contained in the path. That implies we have found a cycle and an arc is removed. It is important to note that we keep track of which paths we still need to continue. These paths that contain the arc that was removed are removed because they are not possible anymore. For the other paths, we continue in the same way. Alternatively, there are no more possibilities for forward vertices. In that case, we just go to the path that is exactly the same as the current path but without the last vertex and add the next forward vertex to that path as the last state of that path. In symbols — suppose the path $(y_{1,i_1}, \dots, y_{k-1,i_{k-1}}, y_{k,i_k})$ has no possible forward vertices anymore, then we take the path $(y_{1,i_1}, \dots, y_{k-1,i_{k-1}}, y_{k,i_{k+1}})$ and try to continue with that. When the path $(y_{1,i_1}, \dots, y_{k-1,i_{k-1}})$ has no forward vertices anymore, we do the same so that eventually we have covered all paths starting from $y_{1,1}$. We do the same for $y_{1,2}$ and so on for every $y_{1,i}$. Every time we encounter a cycle, we remove an arc, discard all unfinished paths that contain this arc, and

then just continue with the remaining unfinished paths.

Once we have found a cycle that does not contain a pattern, we determine what arc needs to be removed. We know that at the start of this algorithm every vertex is in a cycle with a pattern vertex, so we know that for every vertex there is a path to a pattern vertex. We look for a shortest path starting from the given cycle to the pattern. Note that for this path only the first vertex is part of the given cycle. The algorithm to find this shortest path is similar to the one above that finds all possible paths that do not include a pattern. We find paths to the pattern with increasing length starting from the minimal length 2. For each length, we construct the paths starting from each of the vertices of the cycle. The forward vertices in this algorithm are allowed to include the pattern but are not allowed to include any vertex in the cycle. Once one of the forward vertices is the pattern, that path is a shortest path. The arc of the cycle starting from the first vertex of this path to the pattern to the next (the forward) vertex of the cycle is the arc we remove. Note that still for every vertex there is a path to a pattern vertex, so the recognition is not endangered and when we encounter another cycle we can follow the same instructions.

Appendix C: Frenesy

For the general concept of frenesy, we refer to [13, 15]. It suffices here to mention how time-symmetric components in reaction rates (or transition probabilities) allow to modify the population statistics when there is sufficient nonequilibrium driving. In a way that is a realization of what is called the Landauer blowtorch theorem, [25–27]. In other words, when under nonequilibrium conditions, we can change currents and occupations (i.e., steer them) by modifying time-symmetric dynamical activity; see also [28].

We take the simplest example. Suppose we have a cycle, along which there is a uniform driving but we are allowed to choose the time-symmetric part in the transition rates. Suppose a random walk on the ring \mathbb{Z}_m with m vertices and transition rates

$$k(x, x+1) = a_x e^{\varepsilon/2}, \quad k(x+1, x) = a_x e^{-\varepsilon/2} \quad (\text{C1})$$

where $\varepsilon \gg 1$ is the large driving. Then, the stationary distribution is

$$\rho^s(x) \propto \frac{1}{a_x}, \quad x \in \mathbb{Z}_m$$

completely determined (when $\mathcal{E} \gg 1$) by the symmetric factors. Hence, those activities a_x decide the most probable state. That is obviously impossible under detailed balance, when $\varepsilon = 0$. Similar aspects hold then for the expected escape rates and currents.

Appendix D: Examples

1. Disentangling

In Fig. 5 we show an example of a tournament (with patterns $x_1 = 0$ (red square) and $x_2 = 2$ (blue pentagon)). Fig. 6 shows an example of a disentangled system obtained by executing the disentanglement algorithm on the tournament in Fig. 5. We see that for basin B_1 the cycles are $(0, 3, 7, 0)$ and $(0, 3, 7, 5, 0)$ and for B_2 the cycles are $(2, 4, 1, 2)$ and $(2, 6, 4, 1, 2)$.

Let us reconstruct what has happened.

We start with basin B_1 and take the subtournament by removing all vertices that are elements of the other basins. The only other basin is B_2 and it only contains the vertex 2, so we end up with the vertices $\{0, 1, 3, 4, 5, 6, 7\}$. That subtournament is strong because $(0, 3, 4, 5, 6, 1, 7, 0)$ is a Hamilton cycle. Hence, we search for a cycle of length 3 and we find $(0, 3, 7, 0)$. These vertices and the arcs are added to B_1 . Then we go to the other basin B_2 . The subtournament we have to look has the vertices $\{1, 2, 4, 5, 6\}$ because $B_1 = \{0, 3, 7\}$ and that is a strong tournament because $(1, 2, 4, 5, 6, 1)$ is a Hamilton cycle. We search for a cycle of length 3 and find $(2, 4, 1, 2)$ and add these vertices and the arcs to B_2 . We go back to B_1 and take the subtournament with vertices $\{0, 3, 5, 6, 7\}$ and see that it is a strong tournament because $(0, 3, 5, 6, 7, 0)$ is a Hamilton cycle. Now, we look for a cycle of length 4 and find $(0, 3, 7, 5, 0)$ and add these vertices and the arcs to B_1 , which now equals $\{0, 3, 5, 7\}$. Back to B_2 , subtournament with vertices $\{1, 2, 4, 6\}$, which is strong because $(1, 2, 6, 4, 1)$ is a Hamilton cycle, look for a cycle of length 4 and find $(2, 6, 4, 1, 2)$. Add these vertices and the arcs to B_2 , which now equals $\{1, 2, 4, 6\}$. Now, every vertex is an element of one of the basins and there are no cycles that do not contain a pattern, so we stop.

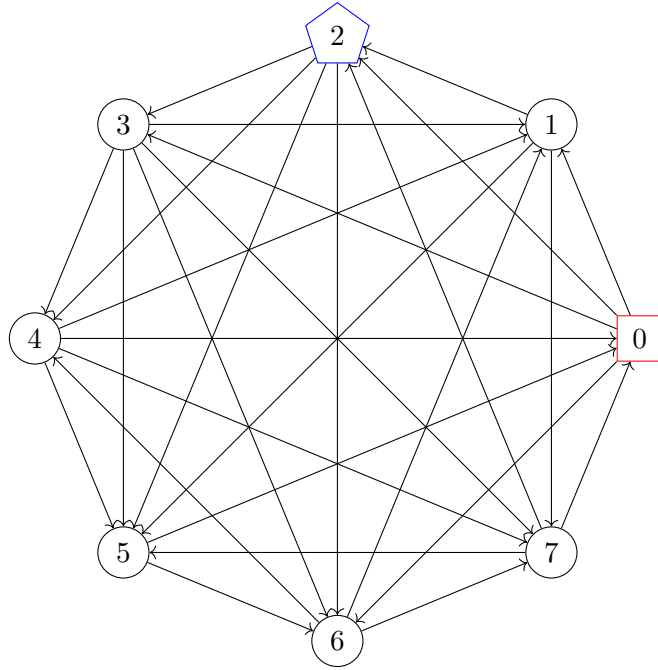


FIG. 5. Example of a tournament and patterns $x_1 = 0$ (red square) and $x_2 = 2$ (blue pentagon).

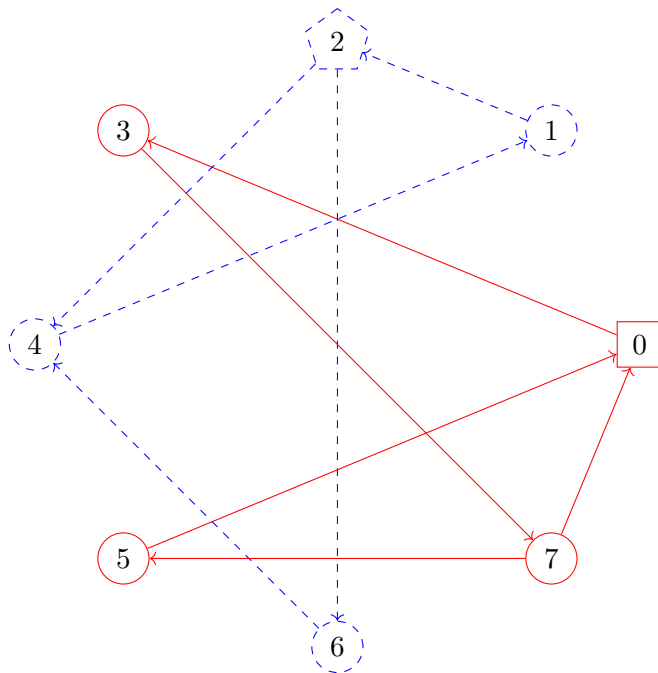


FIG. 6. Example of an oriented graph obtained by executing the disentanglement algorithm on the tournament in Fig. 5. The patterns are $x_1 = 0$ (red square) and $x_2 = 2$ (blue pentagon) and the basins are $B_1 = \{0, 3, 5, 7\}$ (red, full line) and $B_2 = \{1, 2, 4, 6\}$ (blue, dashed line).

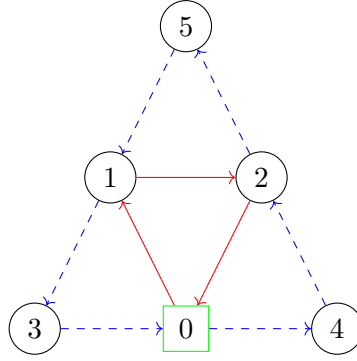


FIG. 7. Example of a cycle outside the pattern where 0 is the pattern (green square). $(0, 1, 2, 0)$ (red, full line) and $(0, 4, 2, 5, 1, 3, 0)$ (blue, dashed line) are cycles that are found by the algorithm and $(1, 2, 5, 1)$ is the cycle outside the pattern.

In the previous example, there are no cycles that do not contain a pattern. Here we want to give an example of what happens in the algorithm that eliminates the cycles that do not contain a pattern; see Fig. 7. 0 is the pattern, $(0, 1, 2, 0)$ (red) and $(0, 4, 2, 5, 1, 3, 0)$ (blue) are cycles that are found by the algorithm (notice that each of them contains the pattern 0 as it should) and $(1, 2, 5, 1)$ is the cycle outside the pattern. For this simple example, we can of course easily find that $(1, 2, 5, 1)$ is the only cycle outside the pattern, but we still want to illustrate how the algorithm finds all the cycles outside the pattern by finding all the possible paths. We do not want to be complete, however. So let us start with the vertex 1. The forward vertices for this vertex are 2 and 3. So we first continue with the path $(1, 2)$. The only forward vertex is 5, so we have the path $(1, 2, 5)$ now. The only forward vertex for 5 is 1, but 1 is already part of the path, so we are lucky and immediately find the cycle outside the pattern $(1, 2, 5, 1)$. Now to find the arc to remove. It is easy to see that $(2, 0)$ is a (and the) shortest path from the cycle to the pattern. The algorithm finds this in the following way. The path length to search for a shortest path from the cycle to the pattern is set to 2 and we start from vertex 1. The only forward vertex from 1 is 3 and we are immediately at the length of the path, so we start with 2, for which the only forward vertex is 0 and that is the pattern, so we have found the path $(2, 0)$ as a shortest path. This means we remove the arc $(2, 5)$. We know that we can stop here but the algorithm does not. The only unfinished path is (1) because both 5 and 2 had only one forward vertex, which we already used up. The unfinished path (1) does not contain the arc $(2, 5)$ so we don't have to remove unfinished paths. The only remaining forward vertex for (1) is 3 and 3 itself does

not have forward vertices so the paths starting from 1 are all found and we take as start vertex 2 now and find all these paths in the same way and continue like that.

2. Path-examples

We give examples here of generated paths on the oriented graph in Fig. 6. We describe the actions that are taken by the frenetic steering algorithm after such a path is generated. We only show the sequence of states of the paths here. We remind the reader that the paths are generated by letting the system evolve until it leaves the state it is in at time T . We do not consider the state the system leaves to after T as part of the path.

Consider $(7, 0, 3)$ as generated path. It leaves a pattern state so that we are in situation (1), and we, therefore, decrease the value of the activity parameter $a(3, 0)$. Consider $(3, 7, 5)$ as generated path. It never visits a pattern state so we are in situation (2), and we, therefore, increase the value of the activity parameters: $a(3, 7)$, $a(7, 5)$ and $a(5, 0)$. Consider $(3, 7, 3)$ as generated path. It never visits a pattern state so we are in situation (2), and we, therefore, increase the value of the activity parameters $a(3, 7)$, $a(7, 0)$ and $a(7, 5)$. Consider as generated path $(3, 7, 0)$ with the actual residence time smaller than the minimal residence time. It never leaves the pattern before time T and is present in the pattern at time T but the actual residence time is smaller than the minimal residence time. We are therefore in situation (3) and we decrease the activity parameter $a(0, 3)$.

If we take 3 as the initial state for a random walk on this system, which is an element of basin B_1 , then a ‘typical’ path, before ‘learning’, would look like the one in Fig. 8. We see that the system does not really care to stay in the pattern $x_1 = 0$. When the learning step is performed, a ‘typical’ path looks like Fig. 9, where we see that the system stays in the pattern once it has arrived there. Note that for such a small basin it is difficult to show the effects of the fast paths.

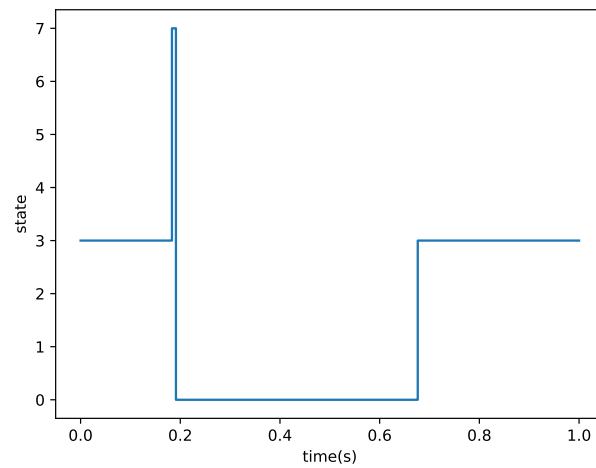


FIG. 8. ‘Typical’ path for a random walker on the disentangled system shown in Fig. 6 when the learning step is not executed yet.

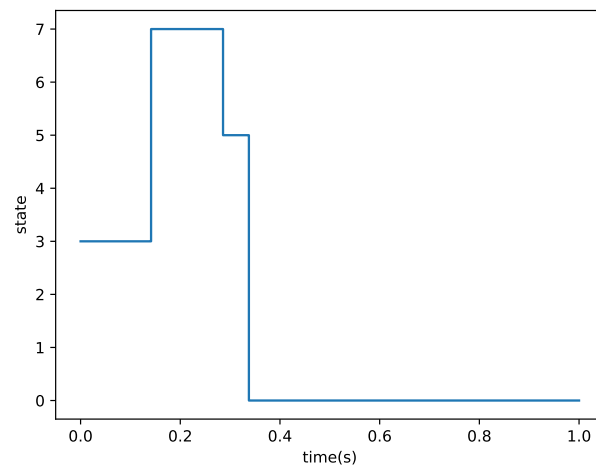


FIG. 9. ‘Typical’ path for a random walker on the disentangled system shown in Fig. 6 when the learning step is executed.

Appendix E: Oscillations in Fig. 2

Here we give an explanation for the oscillations we see in Fig. 2.

One can imagine that for a system with many states, during the algorithm, when the basins are small and when the algorithm looks for a new cycle, the probability is high that

the vertices of the found cycle are all outside the basin. The typical size C_m of such a small basin for which the length of the longest cycle the algorithm has looked for up to then is m , is easily determined:

$$C_m = \sum_{i=2}^{m-1} i = \frac{(m+1)(m-2)}{2} \quad (\text{E1})$$

Also for a system with many states, typically, after the algorithm has finished, the length of the longest cycle the algorithm has looked for is m for some basins and $m+1$ for the other basins, because the probability that a subtournament is strong is very high when the number of states is high. When the number of patterns is also high so that the final sizes of the basins cannot be big, the basins for which the length of the longest cycle the algorithm has looked for is m have typically the same size, as given by E1, and similarly for $m+1$. When the number of states and the number of patterns approach values for which

$$(1 + C_m)k = N \quad (\text{E2})$$

where we view $1 + C_m$ as the typical size of the set including the vertices of a basin for which the length of the longest cycle the algorithm has looked for is m and its associated pattern, then for most of the basins, the length of the longest cycle the algorithm has looked for is m and the size of those basins is C_m . In that case, the average difference in the sizes of the basins is minimal. For a system with a high number of states and a high number of patterns, there are basically ratios between the number of states and the number of patterns that correspond with sizes of basins that are very likely, for which the average difference in the sizes of the basins is minimal. The first members of the sequence defined by $1 + C_m$ are 3, 6, 10, 15 and 21. Now look again at Fig. 2. There we have $N = 1000$. The values for k which correspond to these values for $1 + C_m$ are $1000/3 \approx 333$, $1000/6 \approx 167$, $1000/10 = 100$, $1000/15 \approx 67$ and $1000/21 \approx 48$. We see that these values nicely correspond with the minima in the plot.